



Received: 01-02-2014  
Accepted: 28-03-2014

ISSN: 2321-4902  
Volume 1 Issue 6



Online Available at [www.chemijournal.com](http://www.chemijournal.com)

## International Journal of Chemical Studies

### Red Mud as a Low Cost Adsorbent to Remove Cu(II) ion from Aqueous Solutions

Kumar Sujata <sup>1\*</sup>, Singh D <sup>3</sup>, Mishra A.K <sup>3</sup>, Upadhyay M <sup>2</sup>, Kumar Saroj <sup>3</sup>

1. Department of Chemistry, Kirodimal Institute of Technology Raigarh (C.G), INDIA  
[Email: [skumarrgh@rediffmail.com](mailto:skumarrgh@rediffmail.com)]
2. Department of Chemistry, Dr. C.V. Raman University Bilaspur (C.G), INDIA
3. Department of Chemistry, K. Govt. Arts & Sc. College Raigarh (C.G), INDIA,

---

In the present study, adsorption characteristics of red mud to remove Cu(II) ion from aqueous solutions have been evaluated under batch mode experiments. To have an idea about the nature of adsorption, Freundlich and Langmuir adsorption isotherm models have been discussed. To know the order of reaction Lagergren pseudo first order and pseudo second order equation have been employed and discussed. Intraparticle diffusion model have been discussed to have an idea of the mechanism of adsorption. Spontaneity and feasibility of the process have been discussed using thermodynamic parameters such as change in free energy, change in enthalpy and change in entropy. Activation energy of the process and sticking probability have been calculated and discussed.

---

**Keyword:** Red mud, adsorption, Cu(II) ion, Langmuir isotherm, Lagergren pseudo first-order equation, pseudo-second-order equation.

#### 1. Introduction

Effluents from many industries contain copper and its compounds. These effluents when discharged in nearby river without treatment, they cause pollution to the water and soil which ultimately cause problem to human health as well as environment.

Various methods have been employed and studied to remove heavy metals from aqueous system. However, adsorption method is cheap, easy handling, effective and sludge free. Many substances have been studied as adsorbent along with red mud which is a by-product of aluminium industry. Red mud consists mainly of oxides of Al, Si, Fe, and Ca. These oxides act as active sites for adsorption. Many studies have shown that it can be used as a cheap adsorbent to remove heavy metals from aqueous system <sup>[1-5]</sup>.

In this study, adsorption of Cu(II) ion on red mud has been evaluated as a function of initial copper ion concentration, contact time, temperature, pH

and particle size. For equilibrium studies Langmuir and Freundlich adsorption isotherms have been discussed. For kinetics of adsorption Lagergren pseudo first order equation and pseudo second order equation have been discussed. Thermodynamic parameters along with activation energy and sticking probability have been evaluated and discussed.

#### 2. Material and Methods

Red mud was obtained from BALCO, Korba (C.G). As it is alkaline in nature, it was washed with water till nearly neutral, dried at 105 °C and sieved to get desired particle size. For its characterization and morphology XRF, SEM and FTIR were obtained from SAIF-IIT Bombay. A.R. quality CuSO<sub>4</sub> was used to prepare stock solutions.

In 25 ml of aqueous solution of Cu(II) of given concentration 1.0 g of red mud of desired size was added. It was then agitated in a shaking

machine at desired temperature and pH. After pre-determined time interval, the solution was centrifused, filtered and analyzed for remaining concentration of metal ion by spectrophotometer. Different parameters were: initial metal ion concentration as 25, 50, 75, 100, 125, 150, 175, 200, 225 and 250 mgL<sup>-1</sup> for equilibrium study and 100, 150, 200 and 250 mgL<sup>-1</sup> for rate study; temperature as 303K, 313K and 323K; pH as 2.0, 4.0, 6.5 and 8.0 and particle sizes as 45 μ, 75 μ and 150 μ.

The amount of Cu(II) ion adsorbed was calculated using following mass balance equation [6]:

$$q_e = V (C_i - C_e) / m$$

Where, C<sub>i</sub> and C<sub>e</sub> are Cu(II) ion concentration in mgL<sup>-1</sup>

before and after adsorption respectively, V is the volume of adsorbate in litre, and m is the weight of the adsorbent in grams. The percentage of removal of Cu(II) ion was calculated from the following equation [11]:

$$\text{Removal \%} = 100 (C_i - C_e) / C_i$$

### 3. Results and Discussion

#### 3.1 Characterisation of red mud

Different red mud contain the same basic chemical elements, but in different proportions. Chemical composition of the present red mud obtained from XRF studies are: SiO<sub>2</sub> (43.17%), Al<sub>2</sub>O<sub>3</sub> (13.25%), Fe<sub>2</sub>O<sub>3</sub> (41.20%), CaO (1.09%), MgO (0.73%) and TiO<sub>2</sub> (1.26%).

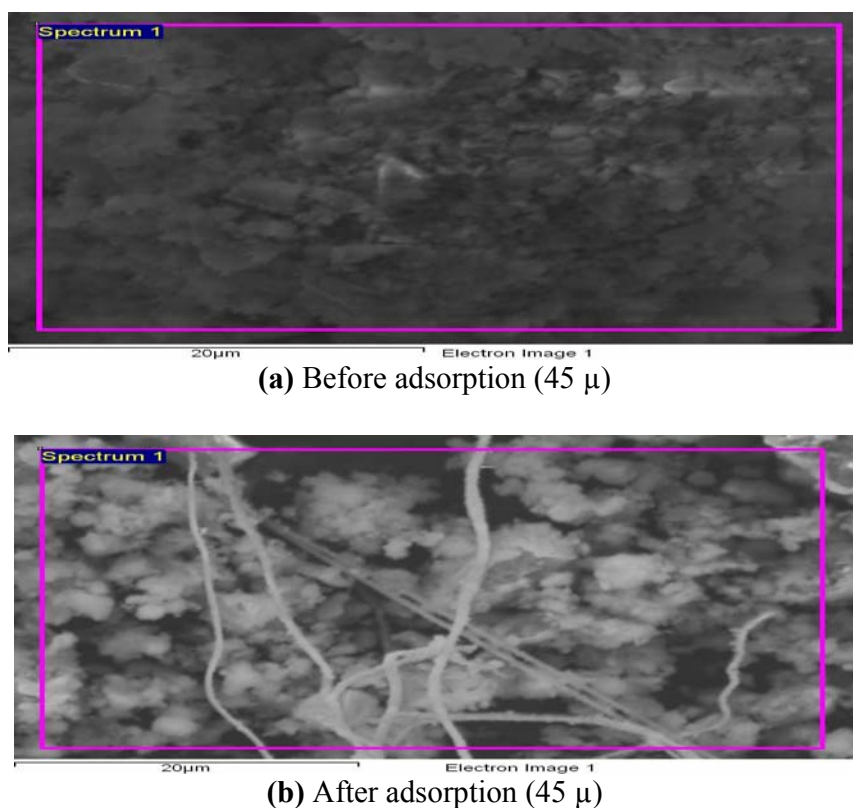


**Fig 1:** (a) is the SEM image of red mud before adsorption and 1(b) after adsorption.

The FTIR spectra of red mud before and after adsorption is shown in figure-2. It shows a broad band around 3500 cm<sup>-1</sup>, which is attributed to surface -OH group of silanol groups (-Si-OH) and

adsorbed water molecules on the surface [7]. A peak around 1400–1600 cm<sup>-1</sup> is attributed to presence of carbonate. A strong peak at 995.22 cm<sup>-1</sup> is due to stretching vibration of Si(Al)-O

group <sup>[8]</sup>. Figure 2(b) shows some new peaks. These additional peaks and variation in

vibrational frequencies indicates that adsorption has taken place on red mud surface.

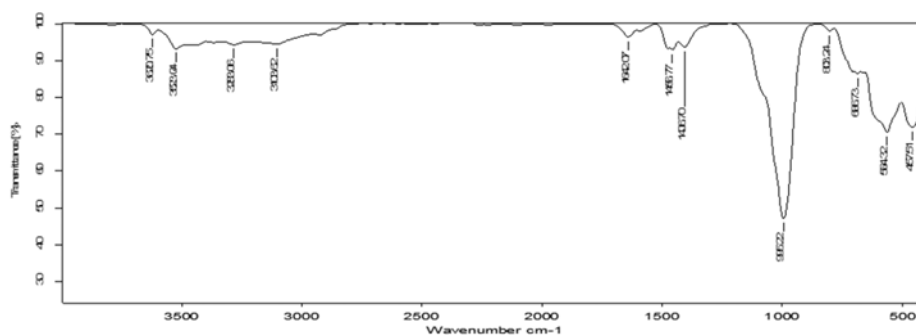


Fig 2(a): FTIR before adsorption

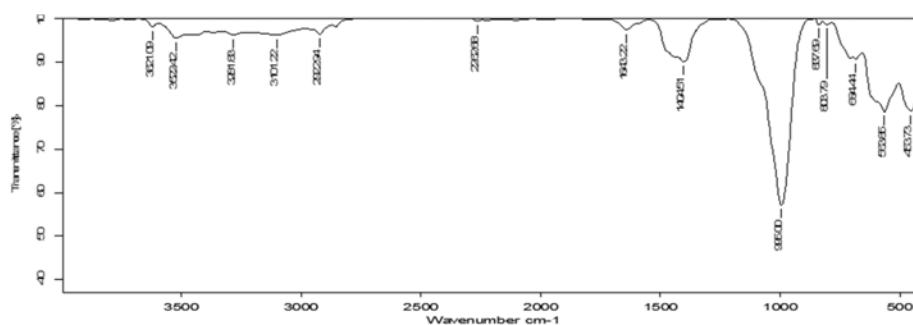


Fig 2(b): FTIR after adsorption

### 3.2 Effect of initial Cu(II) ion concentration

Figure-3 represents percentage removal of Cu(II) ion versus initial metal ion concentration. It is evident that as initial Cu(II) ion concentration increases from 100 mgL<sup>-1</sup> to 250 mgL<sup>-1</sup>, the percentage removal of Cu(II) ion decreases from 79.2% to 70.08%. This may be explained by the fact that adsorbents possess a limited number of active sites and these active sites become saturated at certain concentration.

Figure-4 represents the amount adsorbed at equilibrium  $q_e$  (mgg<sup>-1</sup>) increases with increase in initial metal ion concentration. As initial metal ion concentration increases from 100 mgL<sup>-1</sup> to 250 mgL<sup>-1</sup>, the amount adsorbed increases from 1.98 mgg<sup>-1</sup> to 4.38 mgg<sup>-1</sup>. The reason might be due to the fact that mass transfer resistance of Cu(II) ion between aqueous phase and the solid phase is possibly overcome by the initial metal ion concentration.

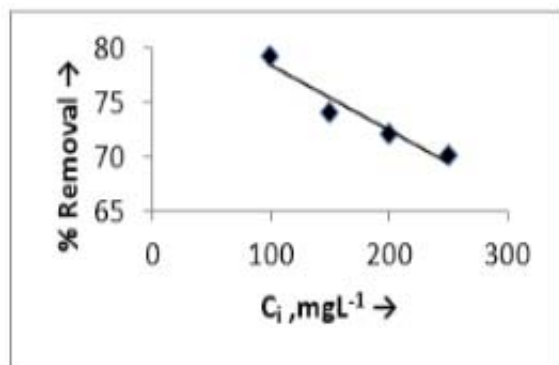


Fig 3: Effect of initial conc. on Cu(II) adsorption

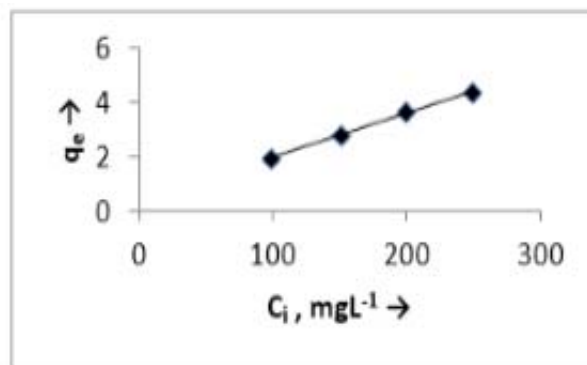


Fig 4: Effect of initial conc. on Cu(II) adsorption

### 3.3 Effect of contact time

Figure-5 represents the effect of contact time on the adsorption of Cu(II) ion on red mud. It is evident that amount adsorbed increases with time and after 120 minutes equilibrium is reached. Initially the rate of adsorption is fast which gradually slows down till equilibrium is reached.

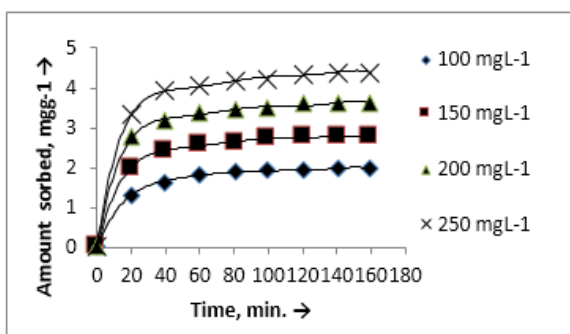


Fig 5: Effect of contact time on adsorption of Cu(II)

### 3.4 Effect of pH

Figure-6 represents the effect of pH on adsorption. By increasing pH from 2.0 to 8.0 the amount adsorbed increases from 1.31  $\text{mgg}^{-1}$  (52.4%) to 2.33  $\text{mgg}^{-1}$  (93.2%). The reason might be due to the fact that at low pH red mud surface acquires positive charge which does not attract  $\text{Cu}^{+2}$  much. At high pH the surface becomes negatively charged and  $\text{Cu}^{+2}$  is adsorbed easily, thereby increasing the amount of adsorption [11].

### 3.5 Effect of temperature

Figure-7 represents the amount of Cu(II) ion

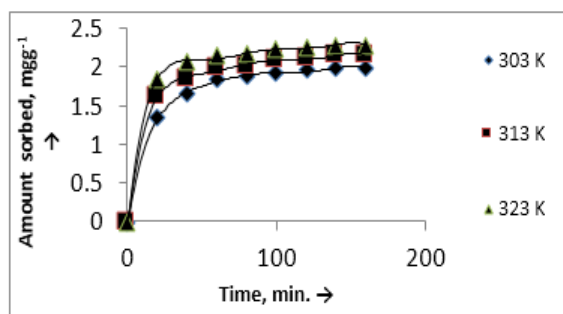


Fig 7: Effect of temperature on adsorption of Cu(II)

The reason might be the fact that initially more number of active sites are present in the red mud and so the rate of adsorption is fast. With increase in time as adsorption progresses, number of active sites decreases and therefore, the rate of adsorption decreases [10].

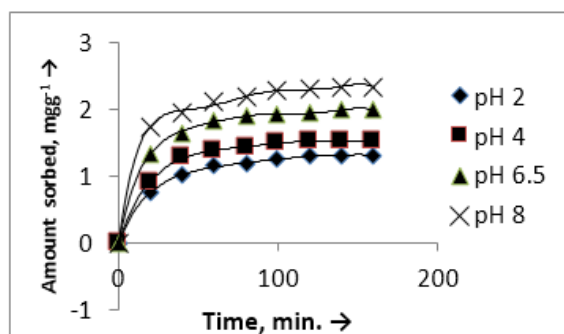


Fig 6: Effect of pH on adsorption of Cu(II) ion

adsorbed with temperature. It is evident that with increase in temperature, the amount adsorbed increases. It increases from 1.98  $\text{mgg}^{-1}$  (79.20%) at 303K to 2.28  $\text{mgg}^{-1}$  (91.2%) at 323K. It indicates the endothermic nature of adsorption. The rate constant of adsorption are  $4.03 \times 10^{-2}$ ,  $5.02 \times 10^{-2}$  and  $6.63 \times 10^{-2}$  per minute at 303K, 313K and 323K respectively indicating that the rate of adsorption increases with increase in temperature. Increase in adsorption with temperature might be due to increase in mobility of ions as well as increase in pore size of the adsorbent.

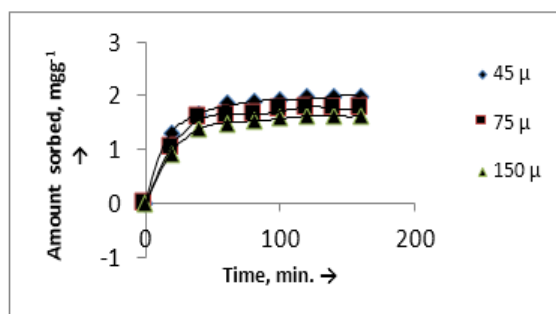


Fig 8: Effect of particle size on adsorption of Cu(II) ion

### 3.6 Effect of particle size

Figure-8 represents the amount of Cu(II) ion adsorbed with particle size. It is evident that as particle size decreases the amount adsorbed increases. The amount adsorbed at 150  $\mu$  is 1.87  $\text{mgg}^{-1}$  (65.20%) which increases upto 1.98  $\text{mgg}^{-1}$  (79.20%) at 45  $\mu$ . The reason might be the fact that as particle size decreases, surface area increases and number of active sites increases thereby increasing adsorption.

### 3.7 Adsorption Isotherm

Langmuir isotherm model assumes adsorption on a homogeneous surface by monolayer adsorption without interaction between the adsorbed molecules [18]. The linear form of Langmuir isotherm [12] is given as:

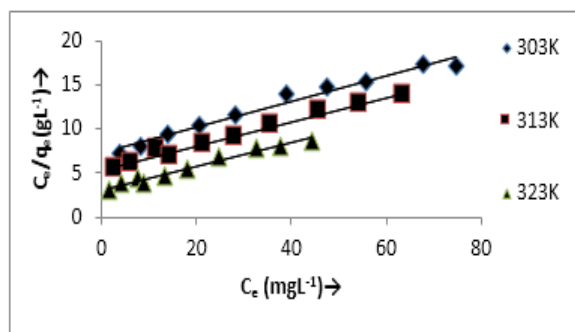


Fig 9: Langmuir isotherm for adsorption of Cu(II)

$$C_e/q_e = 1/\phi \cdot b + C_e/\phi$$

Where,  $q_e$  is the amount of copper adsorbed per gram of the adsorbent at equilibrium,  $C_e$  ( $\text{mgL}^{-1}$ ) is equilibrium concentration of Cu(II) ion in the solution and  $\phi$  and  $b$  are Langmuir constants related to adsorption capacity and adsorption energy respectively. Figure-9 shows the relationship between  $C_e/q_e$  versus  $C_e$ . The plot is linear, indicating the applicability of Langmuir isotherm. Slope and intercept of the straight lines obtained give the value of  $\phi$  and  $b$  respectively and are given in Table- 1. The result shows that the values of  $\phi$  and  $b$  increase on increasing the temperature.

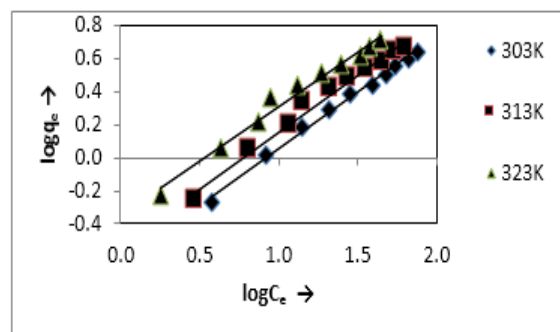


Fig 10: Freundlich isotherm for adsorption of Cu(II)

Table 1: Adsorption isotherm constants for adsorption of Cu(II) on red mud

Langmuir Isotherm Results				Freundlich Isotherm Results		
Temp.(K)	Correlation coefficient, $R^2$	$\phi$	$b$	Correlation coefficient, $R^2$	$K_f$	$n$
303	0.971	6.89	0.019	0.993	0.235	1.47
313	0.987	7.25	0.027	0.984	0.296	1.47
323	0.979	7.58	0.42	0.980	0.444	1.51

To heterogeneous surfaces involving multilayer adsorption, Freundlich adsorption isotherm model can be applied. The linearized Freundlich equation is represented as [13]:

$$\log q_e = \log K_f + 1/n \log C_e$$

Where,  $q_e$  is the amount of Cu(II) ion adsorbed ( $\text{mgg}^{-1}$ ),  $C_e$  is the equilibrium concentration of Cu(II) ion in solution ( $\text{mgL}^{-1}$ ) and  $K_f$  and  $n$  are

constants for the adsorption capacity and intensity of adsorption respectively. Plots of  $\log q_e$  versus  $\log C_e$  has been shown in figure-10 and values of  $K_f$ ,  $n$  and  $R^2$  (correlation coefficient) value have been obtained and given in Table-1. The value of  $K_f$  and  $n$  increases with increase in temperature. Comparing  $R^2$  value shows that both isotherms are applicable. However, experimental data fits better in Freundlich equation.

### 3.8 The Lagergren first order kinetic model

The Lagergren pseudo first order rate equation is represented as [14]:

$$\log (q_e - q_t) = \log q_e - k_1.t/2.303$$

Where,  $q_e$  and  $q_t$  are the amounts of Cu(II)

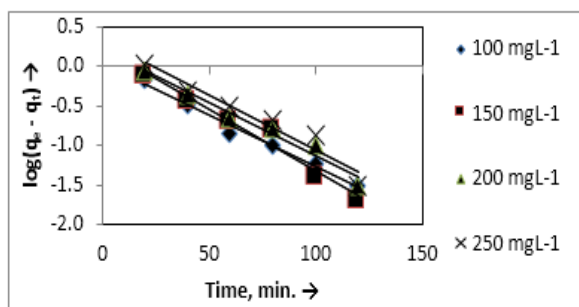


Fig 11: Lagergren pseudo first-order kinetic plot

adsorbed ( $\text{mgg}^{-1}$ ) at equilibrium and at time  $t$ , respectively.  $k_1$  is the Lagergren rate constant ( $\text{min}^{-1}$ ). Figure-11 represents the plot of  $\log(q_e - q_t)$  versus  $t$ . Values of  $q_e$  and  $K_1$  at different initial concentrations have been calculated from the slope and intercept respectively. These values have been given in Table- 2.

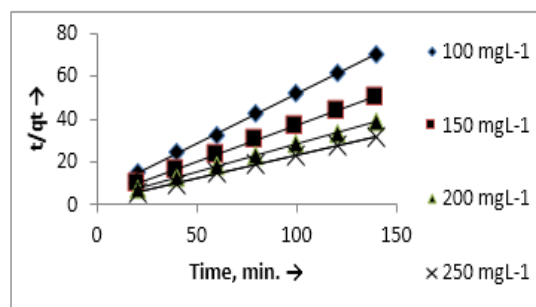


Fig 12: Pseudo-second-order kinetic plot

### 3.9 The pseudo-second-order kinetic model

The adsorption data have been applied to pseudo-second-order kinetic model also which is represented as [15]:

$$t/q_t = 1/K_2.q_e^2 + t/q_t$$

Where,  $K_2$  is the rate constant of second order adsorption ( $\text{g/mg.min.}$ ). Plots of  $t/q_t$  versus  $t$  has been shown in figure-12. Slope and intercept of the graph gives the values of  $K_2$  and  $q_e$  respectively, which have been given in Table- 2.

Table 2: Kinetic parameters for adsorption of Cu(II) ion on red mud

Conc. $\text{mgL}^{-1}$	Lagergren- first- order				Pseudo- second- order			Intraparticle diffusion		
	$K_1$ $\text{min}^{-1}$	$q_{\text{exp}}$ $\text{mgg}^{-1}$	$q_{\text{cal}}$ $\text{mgg}^{-1}$	$R^2$	$K_2$ $\text{g/mg/min}$	$q_{\text{cal}}$ $\text{mgg}^{-1}$	$R^2$	$K_d$ $\text{mg/g.min}^{1/2}$	I	$R^2$
100	$2.76 \times 10^{-2}$	1.98	1.06	0.987	$4.03 \times 10^{-2}$	2.146	0.999	0.095	0.995	0.904
150	$3.45 \times 10^{-2}$	2.78	1.67	0.971	$3.60 \times 10^{-2}$	2.976	0.999	0.111	1.627	0.919
200	$2.99 \times 10^{-2}$	3.61	1.57	0.967	$3.36 \times 10^{-2}$	3.817	0.999	0.123	2.316	0.916
250	$2.99 \times 10^{-2}$	4.38	2.03	0.940	$2.75 \times 10^{-2}$	4.630	0.999	0.146	2.835	0.921

### 3.10 The Intraparticle diffusion model

The Weber and Morris intraparticle diffusion model is expressed as [16]:

$$q_t = K_d . t^{1/2} + I$$

Where, I is the intercept which reflects the

boundary layer effect and  $K_d$  is the intra-particle diffusion rate constant. Figure-13 represents plot of  $q_t$  versus  $t^{1/2}$ . The value of  $K_d$  and I have been calculated from the slope and intercept and are given in Table - 2. As the linear plots did not pass through the origin, it is evident that intraparticle diffusion is not the only rate limiting step [6].

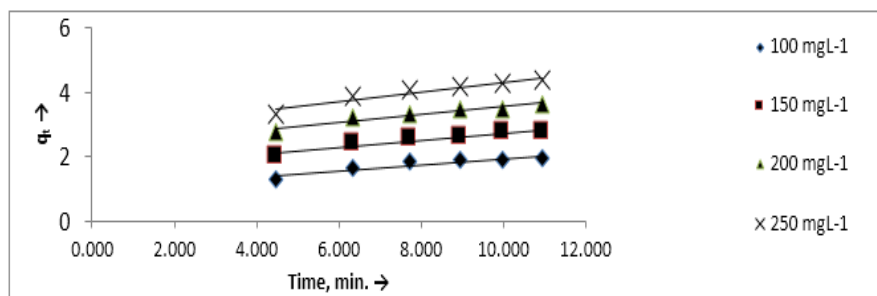


**Fig 13:** Intraparticle diffusion model for adsorption of Cu(II) ion on red mud

It is evident from Table - 2 that  $R^2$  values are higher in the case of pseudo-second-order equation. Moreover,  $q_e$  (cal) values agree better with  $q_e$  (exp) in the case of pseudo-second order reaction showing its applicability over other kinetic model. In general the rate constant  $k_2$  decreases with increase in concentration. The reason might be the possibility that at lower concentration less competition for surface active sites whereas at higher concentration, the competition increases thereby rate constant decreases [17].

### 3.11 Thermodynamic treatment of the adsorption process

Thermodynamic parameters are important in

order to determine the feasibility and spontaneity of the process. Different parameters such as free energy, enthalpy and entropy changes have been calculated using the following equations [24].

$$K_c = C_s/C_e$$

$$\Delta G = -RT \ln K_c$$

$$\log K_c = \Delta S/2.303 R - \Delta H/2.303RT$$

Where,  $C_e$  is the equilibrium concentration in solution in  $\text{mgL}^{-1}$  and  $C_s$  is the equilibrium concentration on the adsorbent in  $\text{mgL}^{-1}$  and  $K_c$  is the equilibrium constant. The Gibbs free energy,  $\Delta G$  was calculated from the above equation. Slope and intercept of the plot between  $\log K_c$  versus  $1/T$  shown in fig 14 gives the values of  $\Delta H$  and  $\Delta S$ . All these values are listed in Table- 3.

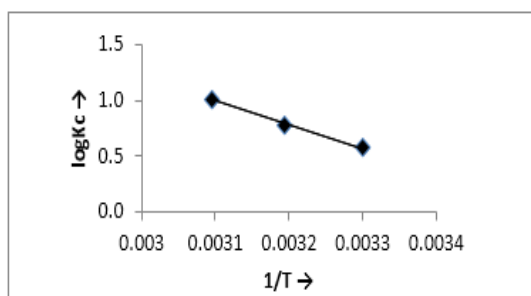


**Fig 14:** Plot of  $\log K_c$  vs  $1/T$

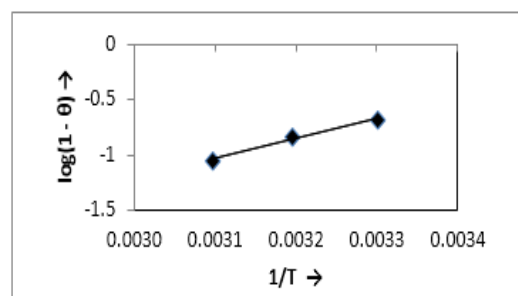


**Fig 15:** Plot of  $\log(1-\theta)$  vs  $1/T$

The values of activation energy ( $E_a$ ) and sticking probability ( $S^*$ ) have been calculated from the experimental data. They were calculated using modified Arrhenius type equation related to surface coverage( $\theta$ ) as follows [19]

$$\theta = (1 - C_e/C_i)$$

$$S^* = (1 - \theta)e^{-E_a/RT}$$

The sticking probability,  $S^*$ , is a function of the adsorbate/adsorbent system under consideration,

depending on temperature and should satisfy the condition  $0 < S^* < 1$ . The values of  $E_a$  and  $S^*$  has been calculated from slope and intercept of the

plot of  $\ln(1-\theta)$  versus  $1/T$  shown in figure-15 respectively and have been given in Table-3.

**Table 3:** Thermodynamic parameters for adsorption of Cu(II) ion on red mud

Temp. K	$\Delta G$ , kJ/mol	$\Delta H$ , kJ/mol	$\Delta S$ , J/mol	$E_a$ , kJ/mol	$S^*$ , J K mol <sup>-1</sup>
303	-3.368	40.67	145.17	34.92	$2.02 \times 10^{-07}$
313	-4.639				
323	-6.280				

Some important conclusions may be withdrawn from the results of Table-3. Negative values of  $\Delta G$  values indicate that the process is spontaneous. Positive  $\Delta H$  value indicates the endothermic nature of adsorption. The positive value of  $\Delta S$  shows the affinity of the adsorbent for the Cu(II) ions. The value of  $E_a$  has been found to be  $34.92 \text{ kJ mol}^{-1}$  for the adsorption. Positive value of  $E_a$  supports the endothermic

nature of the adsorption process. This is in accordance with the positive values of  $\Delta H$ . Since  $S^* \ll 1$ , it indicates that the probability to stick on surface of red mud is very high [20].

#### 4. Mechanism

Speciation [11] of Cu(II) with varying pH has been shown in figure-16.

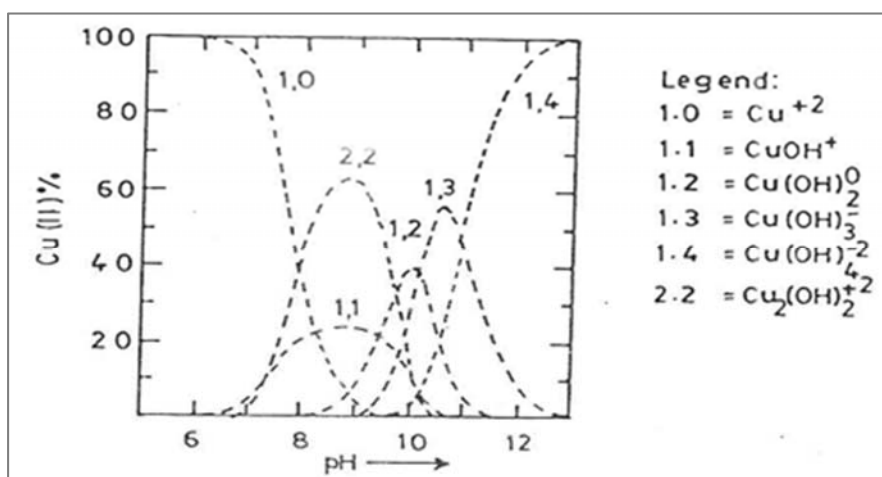
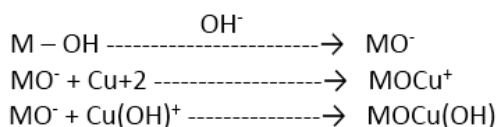


**Fig 16:** Speciation of Cu(II) with varying pH

It is evident that at lower pH, copper is in the form of  $\text{Cu}^{+2}$  and at higher pH it is in the form of  $\text{Cu}(\text{OH})^+$ . It is probable that in acidic medium positively charged surface of adsorbent does not favour the association of cationic adsorbate species. In alkaline medium negatively charged surface offers the suitable sites for the adsorption of  $\text{Cu}^{+2}$  and  $\text{Cu}(\text{OH})^+$  species [21, 22].



Where, M represents the adsorbent surface.

#### 5. Conclusion

It is evident that initial Cu(II) ion concentration, contact time, pH and temperature have marked effect on adsorption. The equilibrium data are best explained by Freundlich adsorption isotherm. Kinetics of adsorption follows second order rate equation. Thermodynamic parameters also favour the adsorption. It is expected that red mud may be used as an efficient adsorbent under suitable conditions.

## 6. Acknowledgement

We are thankful to SAIF, IIT Bombay, for SEM and FTIR analysis of red mud.

## 7. References

- Bhatnagar A, Minocha AK. Conventional and non-conventional adsorbents for removal of pollutants from water – A review. *Indian J Chem Tech* 2006; 13:203-217.
- Karthika C, Sekar M. Removal of Hg(II) ions from aqueous solution by acid acrylic resins: A study through adsorption isotherms analysis. *I Res J Environment Sci* 2012; 1(1):34-41
- Singh D, Singh A. Chitosan for the removal of chromium from waste water. *I Res J Environment Sci* 2012; 1(3):55-57.
- Nadaroglu H, Kalkan E. Removal of cobalt(II) ions from aqueous solutions by using alternative adsorbent industrial red mud waste material. *Int J Phy Sciences* 2012; 7:1386-1394.
- Mobasherpour I, Salahi E, Asjodi A. Research on the batch and fixed bed column performance of red mud adsorbents for copper removal. *Canadian Chemical Transactions* 2014; 2(1):83-96
- Das B, Mondal NK, Roy P and Chatterji S. Equilibrium, Kinetic and Thermodynamic Study on chromium(VI) removal from aqueous solutions using *Pistia Stratiotes* Biomass. *Chem Sci Trans* 2013; 2(1):85-104.
- John C. Interpretation of Infrared Spectra, A Practical Approach, *Encyclopedia of Analytical Chemistry*, Heyers RA (Ed.), John Wiley & Sons Ltd. Chichester, 2000, 10815–10837.
- Ekrem K *et al.* Bacteria – Modified Red Mud for Adsorption of Cadmium Ions from Aqueous Solutions. *Pol J Environ Stud* 2013; 22(2):417-429.
- Tsai WT, Chen HR. Removal of malachite green from aqueous solution using low-cost chlorella-based biomass. *J Hazard Mater* 2010; 175(1-3):844-849.
- Sarin V, Pant KK. Removal of chromium from industrial waste by using eucalyptus bark. *Bioresource Technol* 2006; 97(1):15-20.
- Brummer GW. *Importance of Chemical Speciation in Environmental Process* (Springer Verlag, Berlin), 1986.
- Bansal M, Singh D, Garg VK, Rose P. Use of agricultural waste for the removal of nickel ions from aqueous solutions: Equilibrium and kinetic studies. *World Acad Sci Eng Technol* 2009; 51:431-437.
- Anirudhan TS, Radhakrishnan PG. Thermodynamics and kinetics of adsorption of Cu(II) from aqueous solutions onto a new cation exchanger derived from tamarind fruit shell. *J Chem Thermodynamics* 2008; 40(4):702-709.
- Lagergren S. About the theory of so-called adsorption of soluble substances, *der Sogenannten adsorption geloster stoffe* *Kungliga Svenska psalka de Miens Handlingar*. 1898; 24:1-39.
- Ho YS, McKay G. The kinetics of sorption of divalent metal ions onto sphagnum moss peat. *Water Res* 2000; 34(3):735-742.
- Weber WJ, Morris JC. Kinetics of adsorption on carbon from solution. *J Saint Eng Div Am Soc Eng* 1963; 89:31-60.
- Kumar PS, Ramakrishnan K, Kirupha SD, Sivanesan S. Thermodynamic and Kinetic studies of cadmium adsorption from aqueous solution onto rice husk. *Braz J Chem Eng* 2010; 27:347.
- Arivoli S, Hema M, Karuppaiah M, Saravanan S. Adsorption of chromium ion by acid activated low cost carbon-Kinetic, Mechanistic, Thermodynamic and Equilibrium studies. *E Journal of Chemistry* 2008; 5(4):820- 831.
- Senthilkumar P, Ramalingam S, Sathyaselvabala V, Kirupha DS, Sivanesan S. Removal of copper (II) ions from aqueous solution by adsorption using cashew nut shell. *Desalination*. 2011; 266(1-3):63-71.
- Nevine KA. Removal of direct blue-106 dye from aqueous solution using new activated carbons developed from pomegranate peel: Adsorption equilibrium and kinetics. *J Haz Mat* 2009; 165(1-3):52-62.
- Singh D, Rawat NS. Bituminous coal for the Removal of Cd rich water. *Ind J Chem Technol* 1994; 1:266-270.
- Singh D, Rawat NS. Sorption of Cu(II) by bituminous coal. *Ind J Chem Technol* 1995; 2:49-50.